Manganese(II) Zero-Field Interaction in Cambialistic and Manganese Superoxide Dismutases and Its Relationship to the Structure of the Metal Binding Site

5 AUTHORS, INCLUDING:

Leandro C Tabares
Atomic Energy and Alternative Energies Com…
25 PUBLICATIONS   612 CITATIONS

SEE PROFILE

Néstor Cortez
National University of Rosario and National S…
37 PUBLICATIONS   493 CITATIONS

SEE PROFILE

by Hiraoka
Matsumoto Dental University
45 PUBLICATIONS   771 CITATIONS

SEE PROFILE

Fumiyuki Yamakura
Juntendo University
102 PUBLICATIONS   1,624 CITATIONS

SEE PROFILE

Manganese(II) Zero-Field Interaction in Cambialistic and Manganese Superoxide Dismutases and Its Relationship to the Structure of the Metal Binding Site

Sun Un,*,† Leandro C. Tabares,‡ Néstor Cortez,‡ B. Yukihiro Hiraoka,§ and Fumiyuki Yamakura‖

Contribution from the Service de Bioénergétique, DBJC, CNRS URA 2096, CEA Saclay, 91191 Gif-sur-Yvette, France, Instituto de Biología Molecular y Celular de Rosario (IBR), Universidad Nacional de Rosario and CONICET, Suipacha 531, S20002LRK Rosario, Argentina, Institute for Oral Science, Matsumoto Dental University, Shiojiri 399-0781, Japan, Department of Chemistry, School of Medicine, Juntendo University, 1-1 Hiragagakuendai, Chiba 2701695, Japan

Received June 4, 2003; E-mail: sun@ozias.saclay.cea.fr

Abstract: The Mn(II) high-magnetic-field electron paramagnetic resonance (HFEPR) spectra of five different superoxide dismutases (SODs) were measured at 190 and 285 GHz. The native *E. coli* manganese SOD was found to be distinct from the other SODs by virtue of its large zero-field *E*-value. The two wild-type cambialistic proteins from *Porphyromonas gingivalis* and *Rhodobacter capsulatus* were also distinct. However, the Gly155Thr mutant of the *P. gingivalis* SOD changed the Mn(II) spectrum so that it closely resembled the spectrum of manganese reconstituted *E. coli* iron SOD. This observation paralleled enzyme activity measurements that show that this mutation causes the loss of activity with manganese and enhanced activity with iron indicating a conversion from a cambialistic to an iron-specific protein. The Mn(II) magnetic parameters were determined by simultaneously fitting the multifrequency data. Simulations were carried out by numerically diagonalizing the spin Hamiltonian and explicitly calculating all possible transition probabilities. The relationship between the Mn(II) zero-field interaction and structure of the metal binding site is also discussed.

Introduction

Superoxide dismutases (SODs) are essential for aerobic life, playing an important protective role against oxidative stress. There are four classes of SODs characterized by their metal ion: manganese, iron, nickel, and copper—zinc. A fifth type is active with either manganese or iron and is referred to as being cambialistic.[1-4] The MnSOD, FeSOD, and cambialistic proteins exhibit a high level of structural homology.[5-8] In each case, the metal ligation sphere is five-coordinate with a trigonal
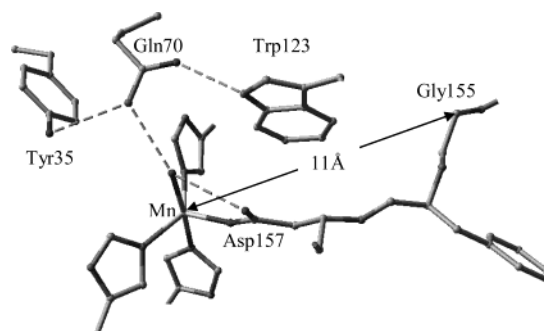

Figure 1. Metal binding site of *P. gingivalis* SOD. The metal ion is bound by His74, His161 and Asp157 in the equatorial plane and by His27 and a solvent molecule at the axial positions. Gly155 is 11 Å (two residues) from the metal ion. The axial solvent molecule hydrogen bonds both Gln70 and Asp157. Gln70 is also hydrogen bonded to Tyr35 and Trp123.

bipyramidal geometry (Figure 1). A solvent (OH^- or H_2O) molecule and a histidine occupy the axial positions and two other histidines and an aspartate (Aps157)[9] occupy the equatorial plane. The solvent molecule donates a hydrogen bond to the aspartate ligand while accepting one from the amide side chain of a nearby glutamine (Gln70). The same glutamine also donates a hydrogen bond to a highly conserved tyrosine residue and

† CNRS URA 2096 and SBE, CEA-Saclay.
‡ Universidad Nacional de Rosario and CONICET.
§ Matsumoto Dental University.
‖ Juntendo University.

(1) Meier, B.; Barra, D.; Bossa, F.; Calabrese, L.; Rotilio, G. *J. Biol. Chem.* **1982**, *257*, 13977−13980.
(2) Amano, A.; Shizukuishi, S.; Tsunemitsu, A.; Maekawa, K.; Tsunasawa, S. *FEBS Lett.* **1990**, *272*, 217−220.
(3) Martin, M. E.; Byers, B. R.; Olson, M. O. J.; Salin, M. L.; Arceneaux, E. L.; Tolbert, C. *J. Biol. Chem.* **1968**, *261*, 9361−9367.
(4) Yamakura, F.; Rardin, R. L.; Petsko, G. A.; Ringe, D.; Hiraoka, B. Y.; Nakayama, K.; Fujimura, T.; Taka, H.; Murayama, K. *Eur. J. Biochem.* **1998**, *253*, 49−56.
(5) Stroupe, M. E.; DiDonato, M.; Tainer, J. A. In *Handbook of Metalloproteins*; Messerschmidt, A., Huber, R., Wieghardt, K., Paulos, T., Eds.; Wiley and Sons: Chicester, 2001; Vol. 2, pp 941−951.
(6) Miller, A.-F. In *Handbook of Metalloproteins*; Messerschmidt, A., Huber, R., Wieghardt, K., Paulos, T., Eds.; Wiley and Sons: Chicester, 2001; Vol. 1, pp 668−682.
(7) Schmidt, M.; Meier, B.; Parak, F. *J. Biol. Inorg. Chem.* **1996**, *1*, 532−541.
(8) Sugio, S.; Hiraoka, B. Y.; Yamakura, F. *Eur. J. Biochem.* **2000**, *267*, 3487−3495.

(9) Amino acid numbering is that of the *P. gingivalis* SOD.

participates in other hydrogen bonds, forming an extensive hydrogen-bonding network that is thought to be important for controlling proton motion and determining the active site pK.[5,6]

One of the intriguing aspects of these three types of SODs is that, despite the high structural homology, enzyme activity is highly metal specific. MnSODs bind but are not active with iron,[10,11] while the reverse is true for FeSOD.[12] Cambialistic SODs exhibit activity with both metals.[1−4] Hence, it is likely that subtle metal−protein interactions make a critical difference in activity. Various spectroscopic techniques have been used to probe metal−protein interactions.[5,6] We have demonstrated that high-field electron paramagnetic resonance spectroscopy (HFEPR) can be an effective tool for studying Mn(II) centers in SODs.[13] In this paper, we have expanded on this earlier work on the HFEPR spectra of *E. coli* MnSOD (EcMnSOD) and manganese reconsituted SOD from *Rhodobactor capsulatus* (RcMnSOD) by including the manganese reconstituted iron SOD from *E. coli* (EcMn(Fe)SOD), the cambialistic SOD from *Porphyromonas gingivalis* (PgMnSOD), and a mutant of the PgMnSOD protein in which glycine-155 has been replaced by a threonine (Gly155Thr-PgMnSOD, Figure 1). Gly155 is conserved in most MnSODs, while in most FeSODs a threonine occupies this position.[4,14] The site is two residues from Asp157, a ligand to the metal ion, and is 11 Å from the metal ion. Yamakura and co-workers have shown that this mutation leads to a 85% reduction in the enzyme activity when the protein is reconstituted with manganese and to an enhanced activity with iron, indicating that this single mutation appears to convert the cambialistic protein to an iron-type protein.[15] Recently, it has been determined that the *Rhodobacter capsulatus* SOD is also cambialistic.[16] Finally, EcFeSOD has long been known to incorporate manganese (EcMn(Fe)SOD), but is inactive with this metal ion.[10,11] The five different proteins provide an important opportunity to test how sensitive the Mn(II) magnetic parameters are to the subtle changes in the protein environment that modulate activity and whether HFEPR spectroscopy can shed any light on the remarkable metal selectivity of SODs.

The Mn(II) EPR spectra of the SOD proteins are determined by the spin Hamiltonian

$$H = \beta \mathbf{B} \cdot \mathbf{g} \cdot \mathbf{S} + \mathbf{I} \cdot \mathbf{A} \cdot \mathbf{S} + \frac{D}{3}(3S_z^2 - S(S+1)) + E(S_+^2 - S_-^2)$$

(1)

where the first term describes the electronic Zeeman interaction and the second the hyperfine interaction between the unpaired electrons ($S = 5/2$) and the manganese nucleus ($I = 5/2$). The last two terms describe the zero-field interaction. In general, all of the terms depend on the orientation of the magnetic field with respect to the Mn(II) site.

The spectra obtained using high microwave frequencies are fundamentally different from those obtained using conventional 9 GHz. Conventional 9 GHz spectra, typified by the RcMnSOD
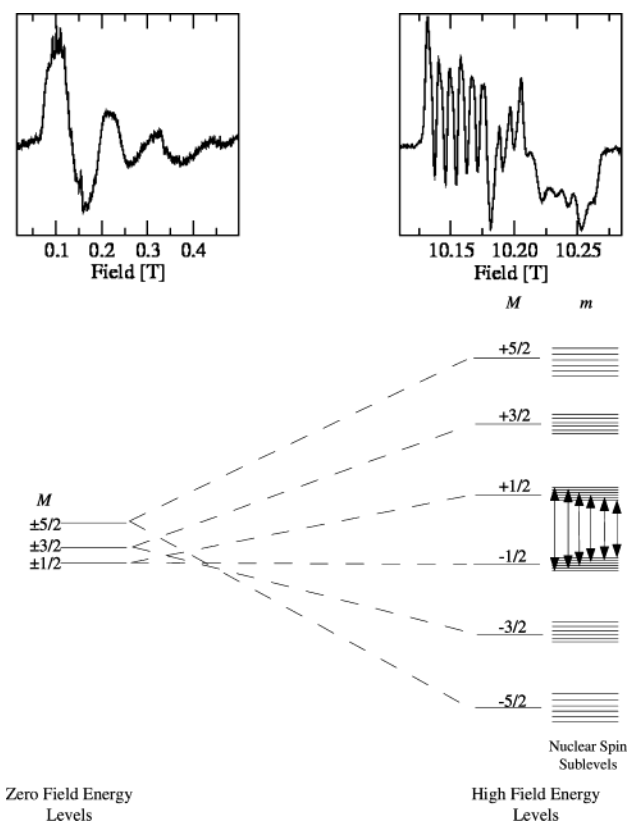

Figure 2. Energy levels of a Mn(II) $S = 5/2$ spin system at zero and high magnetic fields and corresponding RcMnSOD spectra taken at 9 (left) and 285 GHz (right). At 9 GHz, all of the levels contribute to the spectrum. At 285 GHz, the observed spectrum is determined by the $M = -1/2$ to $+1/2$ transitions denoted by the arrows.

shown in Figure 2, are extremely broad, exceeding 0.5 T. This is directly related to the fact that the zero-field interaction of the Mn(II) ions in the trigonal bipyramidal geometry of the SOD is on the order of the microwave frequency.[17] Under this condition, neither the Zeeman nor the zero-field interaction is dominant and all of the six electronic spin states of the $S = 5/2$ manganese ion contribute to the spectrum in a complex manner. Although it is relatively straightforward to understand the overall structure of the spectra,[17,18] simulations and detailed analyses of the spectrum are far from trivial, making it difficult to obtain accurate estimates of the magnetic parameters that define the Mn(II) ions. Recently, Smoukov and co-workers in their study of the FosA protein have detailed an approach to obtaining the Mn(II) magnetic parameters that combines 35 GHz microwave frequency and fast magnetic field sweeps.[19] The primary advantage of this method was the ability to measure directly the zero-field parameters. A different approach is to obtain the spectra at magnetic fields where the Zeeman interaction is much larger than the zero-field interaction. Under this condition, the spectra are much less complex and easier to understand. In large part this comes from the fact that the electronic spin levels become resolved and ordered according to their spin quantum number (Figure 2). Moreover, only the transitions between the $M = -1/2$ and $1/2$ states (where M is the electronic spin quantum

(10) Ose, D. E.; Fridovich, I. *Arch. Biochem. Biophys.* **1979**, *194*, 360−364.
(11) Brock, C. J.; Harris, J. I. *Biochem. Soc. Trans.* **1977**, *5*, 1537−1539.
(12) Yamakura, F. *J. Biochem. (Tokyo)* **1980**, *88*, 191−196.
(13) Un, S.; Dorlet, P.; Voyard, G.; Tabares, L. C.; Cortez, N. *J. Am. Chem. Soc.* **2001**, *123*, 10123−10124.
(14) Cortez, N.; Carrillo, N.; Pasternak, C.; Balzer, A.; Klug, G. *J. Bacteriol.* **1998**, *180*, 5413−5420.
(15) Yamakura, F.; Sugio, S.; Hiraoka, B. Y.; Yokota, T.; Ohmori, D. *Biochemistry* **2003**, *42*, 10790−10799.
(16) Tabares, L. C.; Bittel, C.; Carrillo, N.; Bortolotti, A.; Cortez, N. *J. Bacteriol.* **2003**, *185*, 3223−3227.

(17) Whittaker, M. M.; Whittaker, J. W. *J. Am. Chem. Soc.* **1991**, *113*, 5528−5540.
(18) Wickman, H. H.; Klein, M. P.; Shirley, D. A. *J. Chem. Phys.* **1965**, *42*, 2113−2117.
(19) Smoukov, A. K.; Telser, J.; Bernat, B. A.; Rife, C. L.; Armstrong, R. N.; Hoffman, B. M. *J. Am. Chem. Soc.* **2002**, *124*, 2318−2326.
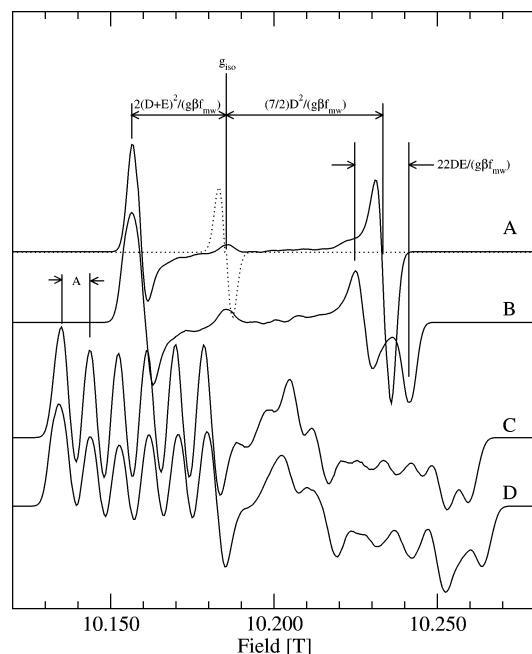
Figure 3. Effect of magnetic parameters on high-field EPR spectrum of a Mn(II) center. The dotted line in trace A is the spectrum in the absence of zero-field and hyperfine interactions ($A = D = E = 0$). The other traces (top to bottom) are (A) $D = 10.5$, $E = 0$, $A = 0$; (B) $D = 10.5$, $E = 0.5$, $A = 0$; (C) $D = 10.5$, $E = 0$, $A = 0.250$ and (D) $D = 10.5$, $E = 0.5$, $A = 0.250$. The field separations between various features denoted in the figure were determined from second-order perturbation formulas.[20]

number) need to be measured. The EPR resonance condition for this transition, derived from the application of perturbation theory, is given by

$$h\nu = \beta g(\theta,\phi)B + A(\theta,\phi)m + \frac{O^2(D,E,A,\theta,\phi)}{g\beta B} + \frac{mO^3(D,E,A,\theta,\phi)}{(g\beta B)^2} \quad (2)$$

where $h\nu$ is the energy of the microwave excitation, m is the nuclear spin quantum number, B is the resonant magnetic field, and the last two terms represent higher order contributions of the zero-field, Zeeman, and hyperfine interactions.[20] For Mn(II) ions, the Zeeman and hyperfine terms are likely to be isotropic with no dependence on orientation of the magnetic field.[21] More importantly, the resonance condition for the $M = -^1/_2$ to $^1/_2$ transition does not depend on the zero-field interaction to first order.[20,22] Therefore, the resonances are expected to be relatively narrow (Figures 2 and 3). By contrast, the transitions between the other states are broadened by the zero-field interactions to first order and are normally difficult to detect (see ref 19 for an alternative method). In fact, the zero-field interaction does broaden the $M = -^1/_2$ to $^1/_2$ transition to second and higher orders (eq 2) and contributes to the line shape of the resonances. Simulation of the line shape can be used to estimate the zero-field parameters. Our approach relies on the use of high magnetic fields not only to simplify the spectrum but also to achieve high resolution in order to obtain the zero-field magnetic

(20) Markham, G. D.; Rao, B. D. N.; Reed, G. H. *J. Magn. Reson.* **1979**, *33*, 592−602.
(21) Griffith, J. S. *The Theory of Transition-Metal Ions*; Cambridge University Press: Cambridge, 1961.
(22) Abragam, A.; Bleany, B. *Electronic Paramagnetic Resonance of Transition Ions*; Clarendon Press: Oxford, 1970.

parameters. We have also enhanced the accuracy of this method by using two very different microwave excitation frequencies.

Experimental Section

Spectrometer. The spectrometer has been described in detail elsewhere.[23] Field calibration was based on a Mn(II) doped MgO standard ($g = 2.001\ 01$),[24] and the absolute error in field measurement is 1 G (0.1 mT) or 0.0001 in g. Unless otherwise mentioned, spectra were obtained with 10−20 G modulation under nonsaturating conditions at 25 K. Resolution of the spectra did not improve with lower modulation fields.

Simulations. Simulations were based on the Hamiltonian given by eq 1. For a given set of g-, A-, D-, and E-values, the Hamiltonian was numerically diagonalized for a small number (<45) of orientations of the magnetic field with respect to the zero-field axes. The resulting eigenvalues and eigenvectors were used to interpolate the values at other orientations. Such an interpolation approach is justified by the Hellmann−Feynmann theorem[25] since the only explicit dependence on the magnetic field comes from the Zeeman term of the Hamiltonian (eq 1). The accuracy of this method was confirmed by comparison to numerical diagonalization results at orientations other than those used as a basis for the interpolation. The powder spectrum was generated by calculating the resonance fields and transition probability for a large number (>100 000) of randomly chosen orientations. For a given orientation, all 36 possible transitions between the $M = -^1/_2$ and $^1/_2$ electronic spin manifolds were taken into account. The resulting histogram, representing the EPR absorption spectrum, was convolved with the derivative of a Gaussian function and scaled relative to the experimental spectrum using linear regression.

Fittings of the spectra were carried out using a standard conjugate gradient minimization approach[26] by minimizing the root-mean-square difference between the experimental and calculated spectra. For all cases, the 285 and 190 GHz data were fit simultaneously.

Sample Preparation. Preparation of RcMnSOD,[14,16] PgMnSOD,[15] and Gly155Thr-PgMnSOD[15] are described separately in other communications. The EcMnSOD sample was obtained commercially (Aldrich-Sigma). The EcMnSOD samples were dissolved in pH 8.0 buffer containing 10 mM Tris and 1 mM EDTA and either dialyzed against the same buffer or washed using a Centricon filter with a molecular weight cutoff of 10 kDa to remove nonspecific Mn(II) contamination. The EcMn(Fe)SOD sample was prepared by reconstitution of *E. coli* FeSOD (Aldrich-Sigma) with manganese using the high-pH procedure of Yamakura using 100 mM CAPS buffer (pH 11).[27]

Unless otherwise mentioned, spectra were obtained between pH 8.0 and 8.5 in 10 mM Tris buffer containing 100 μM to 1 mM EDTA.

Results

Each of the five SODs presented a unique HFEPR spectrum (Figure 4). However, the Mn(II) spectra had several common features. Figure 3 summarizes how the magnetic-field positions of the various features are related to the various magnetic parameters. All of the spectra were centered at a g-value of approximately 2.001 regardless of whether they were obtained at 190 or 285 GHz. This indicated that the electron Zeeman interaction was the dominant interaction above 6 T. The intensity of the 285 GHz spectra reached a maximum at about 25 K, rapidly diminishing with decreasing temperature, indicative of the $M = -^1/_2$ to $^1/_2$ transition. The increase in the spectral width

(23) Un, S.; Dorlet, P.; Rutherford, A. W. *Appl. Magn. Reson.* **2001**, *21*, 341−361.
(24) Burghaus, O.; Plato, M.; Rohrer, M.; Möbius, K.; MacMillan, F.; Lubitz, W. *J. Phys. Chem.* **1993**, *97*, 7639−7647.
(25) Feynman, R. P. *Phys. Rev.* **1939**, *56*, 340−343.
(26) Press, W. H.; Flannery, B. P.; Tenkolski, S. A.; Vetterling, W. T. *Numerical Recipe*; Cambridge University Press: New York, 1986.
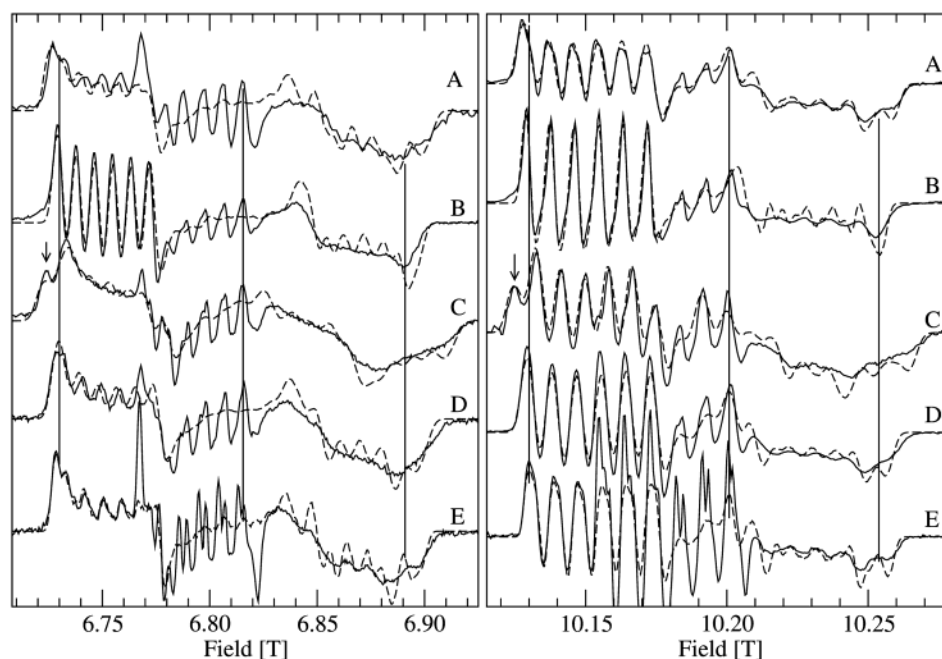(27) Yamakura, F. *J. Biochem.* **1978**, *83*, 849−857.

Figure 4. Experimental Mn(II) HFEPR spectra (solid line) and simulations (dashed) of (A) RcMnSOD, (B) PgMnSOD-WT, (C) EcMnSOD, (D) Gly155Thr-PgMnSOD, and (E) EcMn(Fe)SOD. On the left panel are the 190 GHz spectra and on the right the 285 GHz. The middle vertical lines mark the position of the highest field component of the six-line spectrum arising from nonspecific Mn(II) ions. The arrow indicates the position of the extra feature in the EcMnSOD spectrum resulting from the much larger E-value.

from 0.135 T at 190 GHz to 0.170 T at 295 GHz was clear indication of the higher order zero-field contributions to the line shapes.[20,22] By contrast, the separation between hyperfine features remained independent of microwave frequency. An important aspect of the 285 GHz SOD spectra was the sharpness of the hyperfine features, especially at the low-field edge of the spectra. Since the exact positions of these features are dependent on both D and E (Figure 3), any appreciable variation or distribution in these parameters should have led to broadening of all of these hyperfine features. Hence, the sharpness of these features provided a good indicator of discreteness of these zero-field parameters (see below).

The spectra were composed of a number of hyperfine features, six evenly sharp intense lines at the low-field edge, six sharp variable-intensity lines in the middle, and partially resolved fine structure on the high-field edge. Repeated dialyses of the protein samples against buffer containing EDTA (1 mM) resulted in a decrease in the intensity of the middle set of six lines. The center g-value of these lines was also approximately 2.001. It is likely that some, but not all of the intensity of these six lines were due to nonspecific Mn(II) ions. For this reason, this region of the spectrum was excluded from the fitting procedure described above.

To test how isotropic the g-tensor of the SOD Mn(II) centers was and to obtain an estimate of the g-value required for simulations (see below), we obtained the spectra of EcMnSOD at six different frequencies ranging from 280 to 290 GHz. The resonant magnetic field positions of the six sharp hyperfine features identified in the inset of Figure 5 were monitored as a function of frequency. A saturated ethanol solution of galvinoxyl, an organic radical, was positioned immediately above the frozen protein solution and used as a magnetic-field standard to increase the reliability of the field measurements. The galvinoxyl g-values were determined to be 2.00639, 2.00434, and 2.00244 (absolute error ±0.0001 and relative error ±0.00005)

using the Mn(II) doped MgO standard. The resonant field position of a given feature in the SOD spectrum as a function of microwave frequency is given by eq 2. This equation can be rewritten, ignoring the third-order term, to give

$$(h\nu - Am)B = g\beta B^2 + \frac{O^2(D,E,\theta,\phi)}{g\beta} \tag{3}$$

If the hyperfine contribution Am is known, a plot of $(h\nu - Am)B$ versus βB^2, where B is the resonant magnetic-field position of the feature, will have a slope of g. It can be shown that the first two resolved features in the EcMnSOD spectrum arise from Mn(II) centers for which the magnetic field is orthogonal to the zero-field axis ($\theta = 90°$), with the first corresponding to $(-5/2)A$ and the second to $(-3/2)A$. The three sharp features in the middle of the spectrum arise from a set of orthogonal positions ($\theta = 0°$) with m equal to $+1/2$, $+3/2$, and $+5/2$, respectively. Hence, the g-values of these features compared to those of the low-field lines should give a good estimate of the Mn(II) g-anisotropy. Using the previously determined value of A of 240 MHz,[13] we constructed a plot of the experimental data (Figure 5) using eq 3 that yielded straight lines with slopes of (from low field to high field) 2.000, 1.999, 1.999, 1999, 2.000, and 1.997 for the five hyperfine features. The regression analyses indicated that the g-values obtained in this way were reliable to ±0.002. These direct g-value measurements showed that the Mn(II) g-tensor was isotropic to within the error of the measurement; that is, the Mn(II) g-anisotropy was even smaller than that of the organic galvinoxyl radical.

In the details, the HFEPR spectra of the five SOD proteins were clearly different. The most notable difference was the presence of a sharp low-field feature in the native *E. coli* spectrum (indicated by an arrow in Figure 4) in both the 190 and 285 GHz spectra. The greatest similarity was between the EcMn(Fe)SOD and Gly155Thr-PgSOD spectra (Figure 6), with

Table 1. Summary of HFEPR Simulations[a]

sample	g_{iso}	$|A|$	$|D|$	$|E|$	activity with Mn[b]
RcMnSOD	2.000 92	0.241	10.755 (0.3588)	0.442 (0.0146)	5300[c]
WT-PgMnSOD	2.000 95	0.240	10.680 (0.3562)	0.203 (0.0068)	2653[d]
EcMnSOD	2.001 07	0.239	10.638 (0.3548)	0.928 (0.0305)	4400[e]
Gly155Thr-PgMnSOD	2.000 85	0.243	10.563 (0.3523)	0.345 (0.0115)	304[d]
EcMn(Fe)SOD	2.000 87	0.239	10.510 (0.3506)	0.426 (0.0142)	ND[f]

[a] A, D, and E are given in GHz (and in cm^{-1} in parentheses). [b] In units of (mg of protein)$^{-1}$ (mol of Mn)$^{-1}$ (mol of subunit)$^{-1}$. [c] See ref 16. [d] See ref 15. [e] Commercial source specification (assumes 100% metal content). [f] Not determined, but see ref 10.
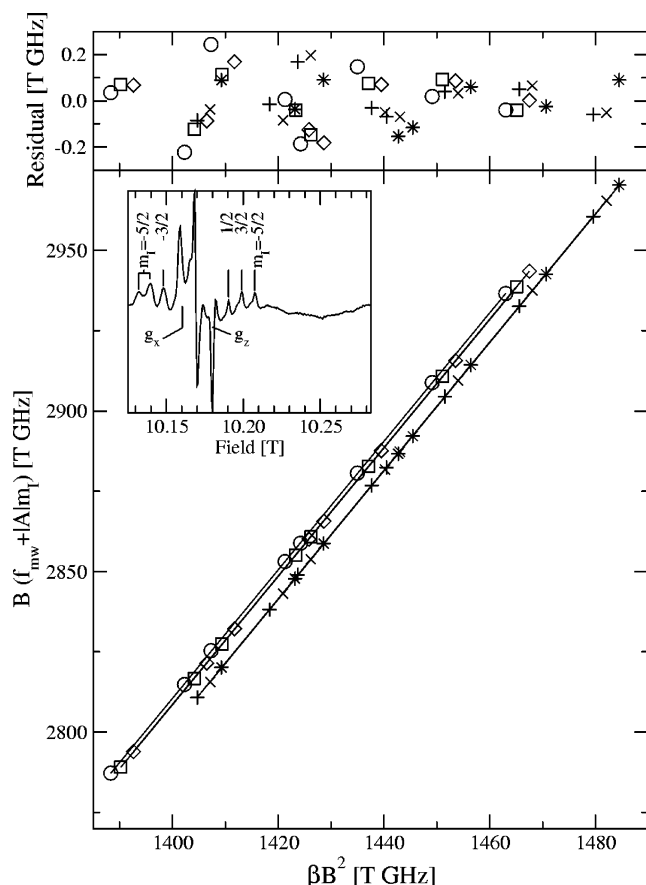

Figure 5. Direct measurement of the g-tensor of the Mn(II) center in EcMnSOD. The resonant field position of six hyperfine features in the inset were monitored as a function of microwave frequency and plotted in the manner described in the text (lower panel). Linear regression yielded g-values (from low to high field): 2.000 (○, $m_I = -5/2$), 1.999 (□, $m_I = -5/2$), 1.999 (◇, $m_I = -3/2$), 1.999 (+, $m_I = 1/2$), 2.000 (×, $m_I = 3/2$), 1.997 (∗, $m_I = 5/2$). The upper panel shows the residuals demonstrating the quality of linear fits.

the latter being slightly wider. To quantitatively analyze the data, simulations were carried out as described above. This analysis differed from our previous work in three ways: 190 GHz data were included in the simulations, all 36 transition probabilities were explicitly calculated, and transition energies were determined from numerical diagonalization of the spin Hamiltonian (eq 1). The spin parameters obtained for the fits are summarized in Table 1, and the fits themselves are shown in Figure 4.

The zero-field D-values for RcMnSOD and EcMnSOD were about 0.3 GHz (0.01 cm^{-1}) higher than those obtained previously, and the E-values were also slightly higher (<0.09 GHz or 0.003 cm^{-1}).[13] The quality of the fits was better using numerical diagonalization compared to the simple perturbation equations, most notably in the high-field edge of the spectra. This improvement could be directly traced to the inclusion of
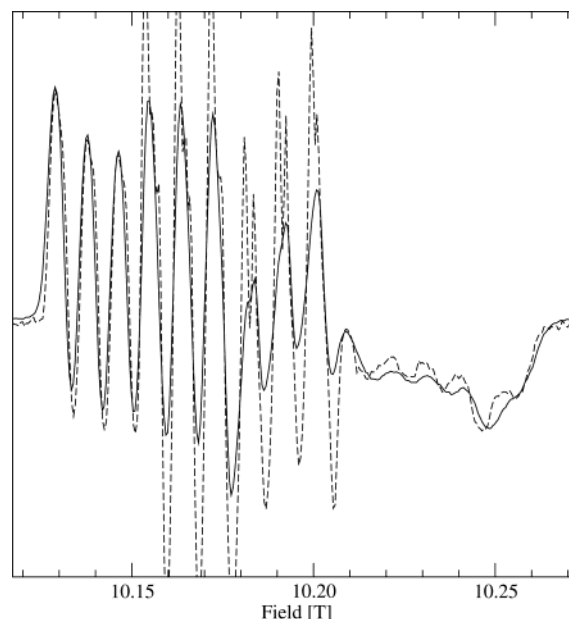

Figure 6. Comparison of the Gly155Thr-PgMnSOD (solid) and EcMn-(Fe)SOD (dashed) Mn(II) HFEPR spectra. The spectra have been vertically scaled to obtain maximum overlap. The largest differences correspond to different amounts of nonspecific Mn(II) in the center of the spectra.

transition probabilities, especially those that are considered formally "forbidden". Bleany and Rubins[28,29] have shown that the relative intensity of the forbidden transitions involving simultaneously excitation of electron and nuclear spins compared to the allowed transition, which excites only the electronic spin, is given by

$$\left(\frac{3D\sin 2\theta}{4g\beta H}\right)^2\left\{1 + \frac{S(S+1)}{3M(M+1)}\right\}^2[I(I+1) - m^2 + m]$$

where S and I are the electron and nuclear spins, respectively, M and m are their respective spin quantum numbers, and θ is the angle between the zero-field axis and the magnetic field. The high-field edge of the spectrum corresponds to centers for which this angle is 45° and is also the region where forbidden transitions are maximal. The highly resolved lower half of the spectrum corresponds to centers for which θ is 0° and 90°. In this region, the forbidden transition probabilities are zero. For a D-value of 10 GHz (0.3 cm^{-1}), the forbidden transitions at 10 T are predicted to be more than half the intensity of that of the allowed. Hence, much of the systematic error which we observed in our previous simulations was a direct consequence of neglecting the forbidden transitions. The presence of these forbidden transitions was also in part responsible for the apparent loss of resolution at the high-field edge of the spectra.

(28) Bleany, B.; Rubins, R. S. *Proc. Phys. Soc. (London)* **1961**, 77, 103−112.
(29) Bleany, B.; Rubins, R. S. *Proc. Phys. Soc. (London)* **1961**, 78, 778.

Even with the inclusion of the forbidden transitions, the high-field edge of the fits did not agree as well as the low-field edge. Inclusion of cubic zero-field terms (data not shown) did not yield any improvements. Since most SOD structures are either dimers or tetramers, we also considered dipolar coupling between Mn(II) centers. The PgSOD crystallographic data (PDB accession code: qnn) indicate that the shortest Mn interspin distance was about 18 Å. On the basis of the work of Käss and co-workers,[30] we estimated that spectral features would only shift by about 5 G (0.5 mT), clearly an insufficient effect to explain the observed discrepancies in the fits. As discussed above, field positions of the various features are defined by *A*, *D*, and *E* (Figure 3). Consequently, the presence of well-defined sharp hyperfine features argued against distributed spin parameters as the origin of the differences between the experimental and simulated spectra. If the magnetic parameters were distributed, this should have also led to a more uniform systematic error rather than the observed field-dependent error. Despite this small systematic error in the simulations, the combination of multifrequency data and relatively large number of spectral features allowed us to have a high level of confidence in the magnetic parameters.

There were several clear trends in these magnetic parameters. The hyperfine couplings were essentially identical for all five proteins with a value 0.241 GHz. The isotropic *g*-values were identical to within the uncertainty in magnetic field calibration (±0.0001), with an average value of 2.00091 and a standard deviation of 0.00011. This value is consistent with the directly measured value of 2.000 ± 0.002 (Figure 5). The *E*-values showed no discernible trend, except for the fact that the EcMnSOD value was distinctly larger. The two proteins with low or no activity with Mn(II) (EcMn(Fe)SOD and Gly155Thr-PgSOD) exhibited the lowest *D*-values. Although the total variation in *D*-values was small, the differences were significant. The differences in the zero-field parameters are visually discernible in both the 285 and 190 GHz spectra (Figure 4). Moreover, when the *D*-value obtained for Gly155Thr-PgMn-SOD was used as the starting point for the fitting of the wild-type spectra, the wild-type values were returned. The converse was also true. Error analysis of the fitting procedure indicated errors of ±0.0020 cm^{-1} or 0.060 GHz in the zero-field values.

Discussion

It is interesting to compare the size of the SOD zero-field parameters with those of other Mn(II) centers. Tetrahedral and octahedral Mn(II) complexes with iodide and bromide ligands have some of the largest Mn(II) *D*-values, ranging from 15 to 27 GHz.[31,32] These large values appear to be associated with the presence of the large halides, since the corresponding chloride complexes with similar geometries have significantly smaller *D*-values (about 5 GHz). Numerous measurements indicate that octahedral Mn(II) centers with oxygen and nitrogen ligands have relatively small *D*-values (≤2 GHz).[33] Two such protein-based examples are concanavalin A with a *D*-value of only ∼0.9 GHz at 4.5K[34] and the azide complexed EcMnSOD

and RcMnSOD with *D*-values of 1 and 2 GHz, respectively.[13] By contrast, the much larger values measured for the Mn-containing SODs and the fosfomycin-bound FosA enzyme (*D* = 8.4 GHz or 0.28 cm^{-1}) by Smokov and co-workers appear to be intrinsic to the five-coordinate geometry.[19] To go beyond such qualitative comparisons, it is necessary to understand the underlying interactions that are responsible for the zero-field interaction and their dependence on molecular structure.

The zero-field interaction in d^5 ions has been studied since 1934.[35] For Mn(II) ions, there appears to be only two significant contributions, spin−orbit coupling and spin−spin interactions.[21,36,37] For the free ion, both contributions are, to first order, zero since the Mn(II) electronic ground state is spherically symmetric.[21] Therefore, the magnitude of the zero-field parameters gives a measure of the deviation from spherical symmetry due to the surrounding ligands. In the case of octahedral (six-coordinate) and tetrahedral (four-coordinate) Mn(II) ions, the empirical superposition model (SPM) has been used to quantitatively relate the size and sign of zero-field parameters to the structure of the Mn(II) ligand environment.[33,38] In the SPM, the individual ligand contributions to the *D*- and *E*-values are additive. Each contribution is the product of three terms: an empirical factor depending on chemical identity of the ligand atom, a trigonometric angle factor depending on the angular position of the ligand, and an r^{-7} dependent term that takes into account the ligand−metal distance.[33,39] Hence, there is good evidence that Mn(II) zero-field parameters can be very sensitive to molecular structure. At a phenomenological level, this high sensitivity is clearly demonstrated by our comparative study. Ostensibly homologous structures yield different HFEPR spectra. The effect of the Gly155Thr mutation on the PgSOD spectrum is also a good example of this.

As described in the Introduction, glycine-155 is highly conserved in MnSODs, including EcMnSOD, and is present in the cambialistic proteins, PgSOD and RcSOD, but is a threonine in most FeSODs.[4,14] Yamakura and co-workers have very recently shown that a mutation of this glycine in PgSOD to a threonine significantly reduces enzymatic activity with manganese and increases activity with iron, reflecting a conversion from a cambialistic to nearly an iron-specific SOD.[15] This conversion was also apparent in the Mn(II) HFEPR spectra. Although the HFEPR spectrum of the wild-type PgSOD is distinct from others, the Gly155Thr mutation modifies the PgMnSOD spectrum so that it closely resembles that of the *E. coli* EcMn(Fe)SOD. This implies that the manganese−protein interactions in the mutant must be similar to those in EcMn-(Fe)SOD and distinct from those in the three active SODs.

The main effect of the mutation of Gly155 to a threonine in PgSOD was the displacement of the adjacent Trp123 toward Gln70 and the elongation of the hydrogen bond between the Gln70 and solvent by 0.36 Å (Figure 1).[15] However, to within statistical uncertainty, the geometry about the metal-binding site was unaffected by the mutation, indicating the possibility that changes in hydrogen bonding and protein electrostatics beyond the primary ligand shell may have been responsible for the

(30) Käss, H.; MacMillan, F.; Ludwig, B.; Prisner, T. F. *J. Phys. Chem. B* **2000**, *104*, 5362−5371.
(31) Wood, R. W.; Stucker, D. M.; Jones, L. M.; Lynch, W. B.; Misra, S. K.; Freed, J. H. *Inorg. Chem.* **1999**, *38*, 5384−5388.
(32) Goodgame, D. M. L.; El Mkami, H.; Smith, G. M.; Zhao, J. P.; McInnes, E. J. L. *Dalton Trans.* **2002**, 34−35.
(33) Heming, M.; Remme, S.; Lehmann, G. *J. Magn. Reson.* **1986**, *69*, 134−143.

(34) Carmieli, R.; Manikandan, P.; Epel, B.; Kalb, A. J.; Schnegg, A.; Savitsky, A.; Mobius, K.; Goldfarb, D. *Biochemistry* **2003**, *42*, 7863−7870.
(35) Van Vleck, J. H.; Penney, W. G. *Philos. Mag.* **1934**, *17*, 961−969.
(36) Pryce, M. H. L. *Phys. Rev.* **1950**, *80*, 1107−1108.
(37) Chakravarty, A. S. *J. Chem. Phys.* **1963**, *39*, 1004−1011.
(38) Remme, S.; Lehmann, G. *Chem. Phys. Lett.* **1985**, *1985*, 318−320.
(39) Newman, D. J.; Urban, W. *Adv. Phys.* **1975**, *24*, 793−844.

observed modification in the Mn(II) zero-field interaction. Alternatively, the differences in the HFEPR spectra could have been due to structural changes to the primary ligand sphere too small to be detected by crystallography. This could very well be the case if Mn(II) ions with five-coordinate geometries are as sensitive to ligand−metal distance as those with six- and four-coordinate geometries.[33] Ultimately, it seems somewhat unlikely that changes in electronic environment and primary ligand sphere geometry are completely unrelated. In either case, it would be reasonable to conclude that these interactions have been modified by the Gly155Thr mutation of the PgMnSOD protein so that they resemble those in EcMn(Fe)SOD.

Mn(II) high-field EPR appears to be an extremely sensitive probe of the electronic structure of the Mn(II) ion in SODs. These results on the SODs suggest the possibility that the different types of SODs can be discriminated by their HFEPR spectrum. Ultimately, the question we wish to pursue is whether protein interactions which determine the Mn(II) zero-field interaction also play a role in protein function and the distinct metal specificity of superoxide dismutases.